Supporting Information

Table of contents **Pages**

X-ray crystallography

Crystal data and collection details for **1'** and **tpm^{IBU}** are reported in Table S1. Data were recorded on a Bruker APEX II diffractometer equipped with a PHOTON2 detector using Mo–Kα radiation. Data were corrected for Lorentz polarization and absorption effects (empirical absorption correction SADABS).[1] The structure was solved by direct methods and refined by full-matrix least-squares based on all data using F^2.[2] Hydrogen atoms were fixed at calculated positions and refined by a riding model. All non-hydrogen atoms were refined with anisotropic displacement parameters.

Table S1. Crystal data and measurement details for **1'** and **tpm^{IBU}**

	1'	**tpm^{IBU}**
Formula	$C_{20}H_{20}F_{12}FeN_{12}P_2$	$C_{24}H_{28}N_6O_2$
FW	774.27	432.52
T, K	100(2)	100(2)
λ, Å	0.71073	0.71073
Crystal system	Monoclinic	Monoclinic
Space group	$P2_1/n$	$P2_1/n$
a, Å	7.5010(6)	13.0977(7)
b, Å	16.7642(14)	8.4764(5)
c, Å	11.2100(10)	20.6292(11)
β,°	93.792(3)	94.579(2)
Cell Volume, Å^3	1406.6(2)	2283.0(2)
Z	2	4
D_c, g·cm^{-3}	1.828	1.258
μ, mm^{-1}	0.769	0.083
F(000)	776	920
Crystal size, mm	0.16×0.14×0.12	0.25×0.21×0.19
θ limits,°	2.189-26.999	1.981-26.999
Reflections collected	20477	32182
Independent reflections	3058 [R_{int} = 0.1443]	4906 [R_{int} = 0.0412]
Data / restraints /parameters	3058 / 0 / 214	4906 / 0 / 292
Goodness on fit on F^2	1.130	1.103
R_1 ($I > 2\sigma(I)$)	0.0638	0.0498
wR_2 (all data)	0.1434	0.1157
Largest diff. peak and hole, e Å^{-3}	0.968 / –0.711	0.416 / –0.257

Figure S1. View of the X-ray structure of $[Fe(\kappa^3\text{-tpm})_2][PF_6]_2$, **1'**. Displacement ellipsoids are at the 50% probability level. Selected bond lengths (Å) and angles (°): Fe(1)-N(1) 1.962(3), Fe(1)-N(3) 1.962(3), Fe(1)-N(5) 1.969(3), N(1)-N(2) 1.365(5), N(3)-N(4) 1.366(5), N(5)-N(6) 1.362(5), N(2)-C(10) 1.439(5), N(4)-C(10) 1.437(5), N(6)-C(10) 1.439(6), N(1)-Fe(1)-N(3) 87.66(14), N(1)-Fe(1)-N(5) 86.95(14), N(3)-Fe(1)-N(5) 88.29(14), N(1)-Fe(1)-N(1)^i 180.0, N(3)-Fe(1)-N(3)^i 180.0, N(5)-Fe(5)-N(5)^i 180.0, N(2)-C(10)-N(4) 109.8(3), N(2)-C(10)-N(6) 109.7(3), N(4)-C(10)-N(6) 109.7(3). Atoms labelled A(X)^i have been generated by symmetry operation: -x+1, -y+1, -z+2.

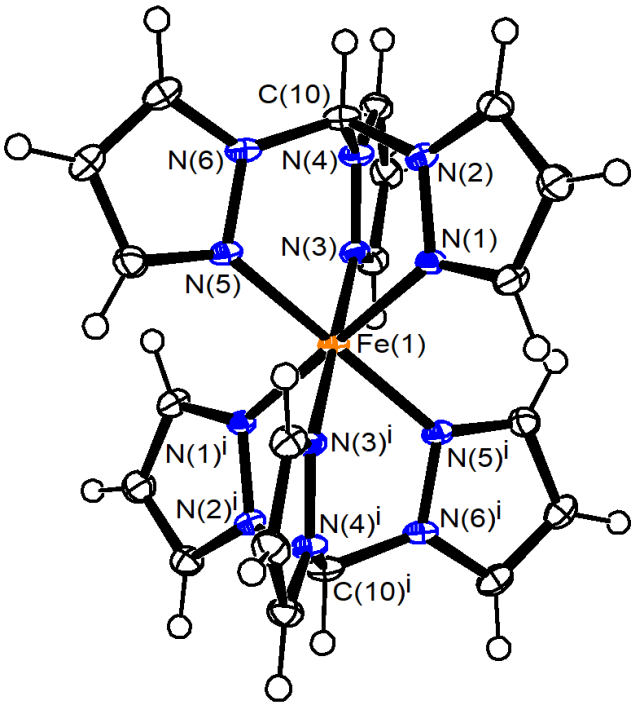

IR spectra

Figure S2. Solid-state IR spectrum (650-4000 cm^{-1}) of **Tpm^{OH}**.

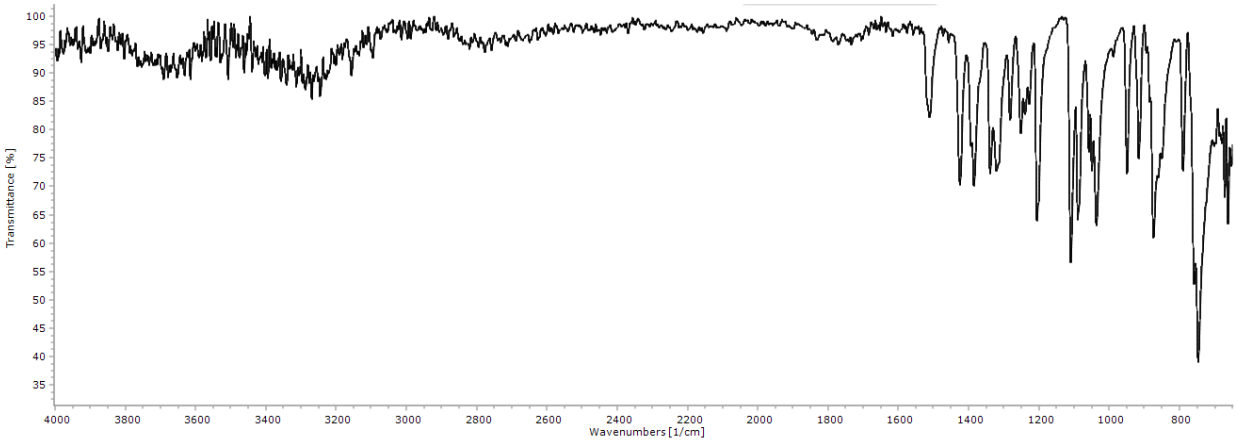

Figure S3. Solid-state IR spectrum (650-4000 cm^{-1}) of **Tpm^{IBU}**.

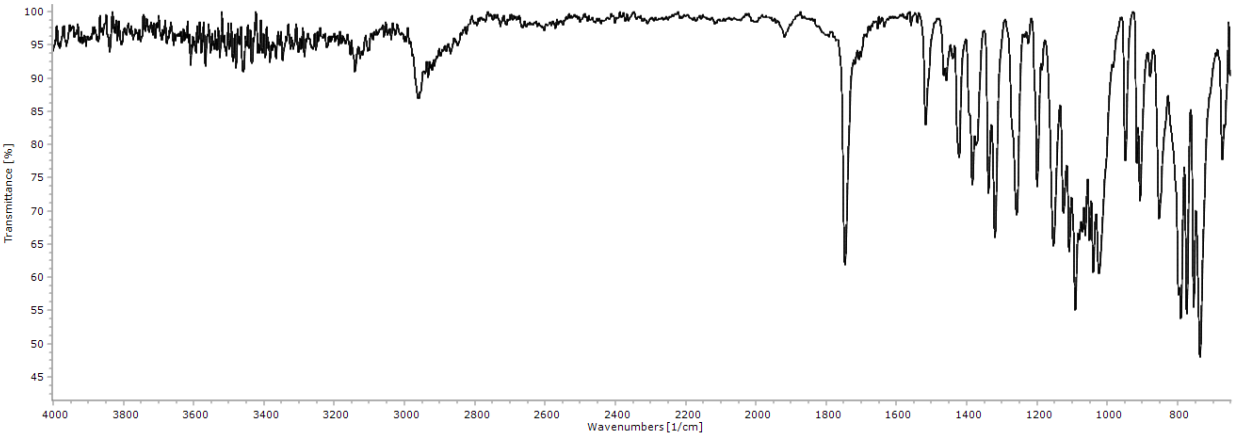

Figure S4. Solid-state IR spectrum (650-4000 cm^{-1}) of **Tpm^{FLU}**.

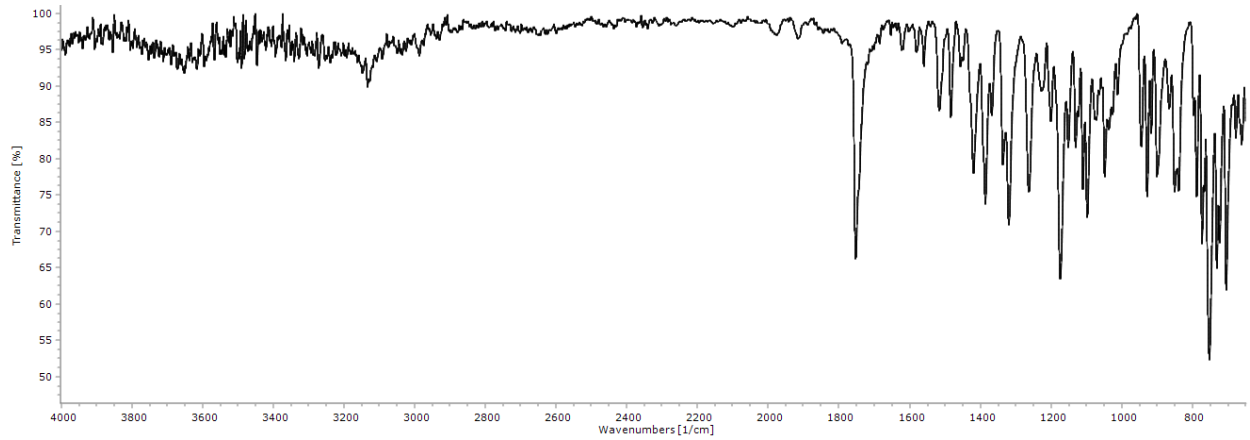

Figure S5. Solid-state IR spectrum (650-4000 cm^{-1}) of **1.**

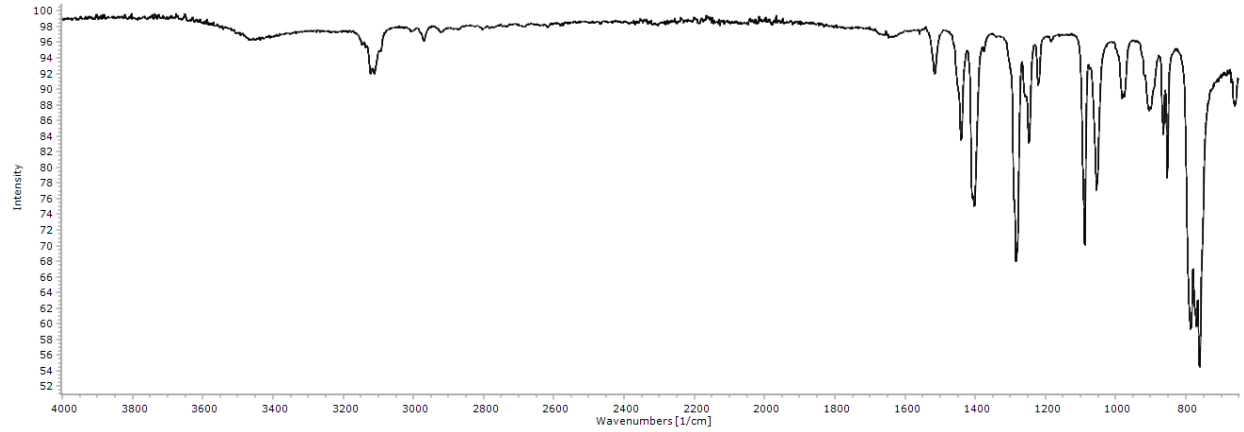

Figure S6. Solid-state IR spectrum (650-4000 cm^{-1}) of **2.**

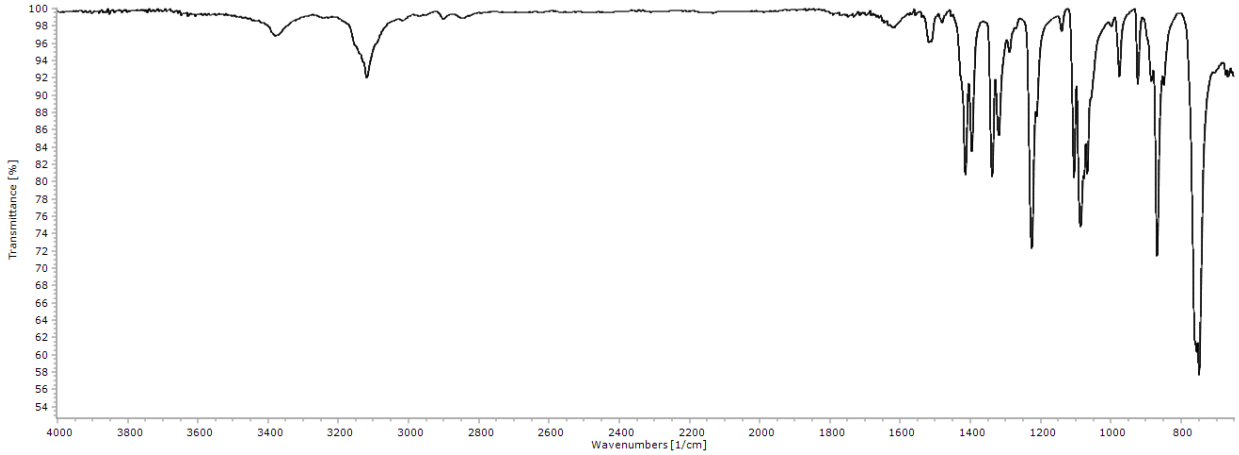

Figure S7. Solid-state IR spectrum (650-4000 cm^{-1}) of **3.**

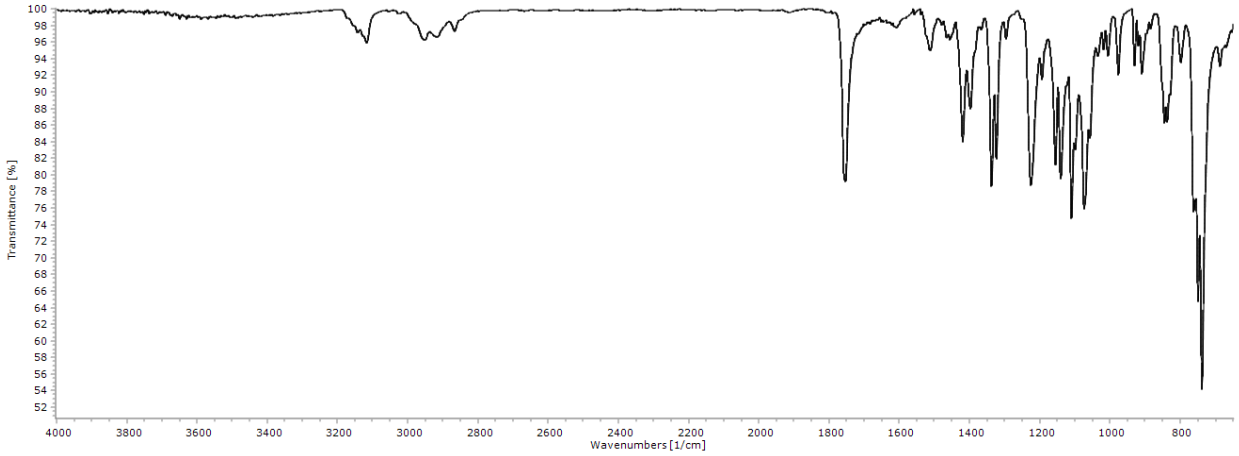

Figure S8. Solid-state IR spectrum (650-4000 cm^{-1}) of **4.**

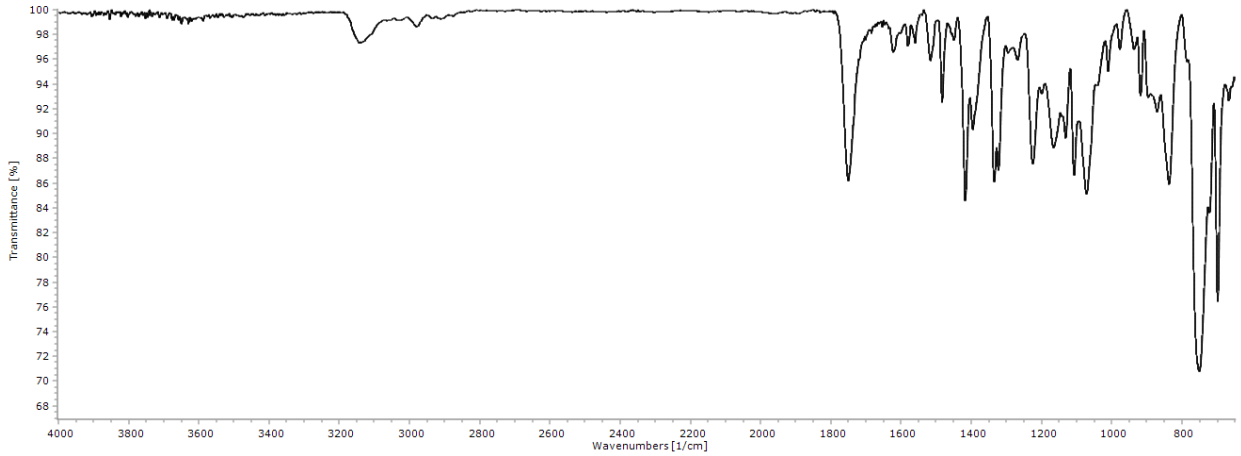

NMR spectra

Figure S9. ^{1}H NMR spectrum (401 MHz, $CDCl_3$) of **Tpm^{IBU}**.

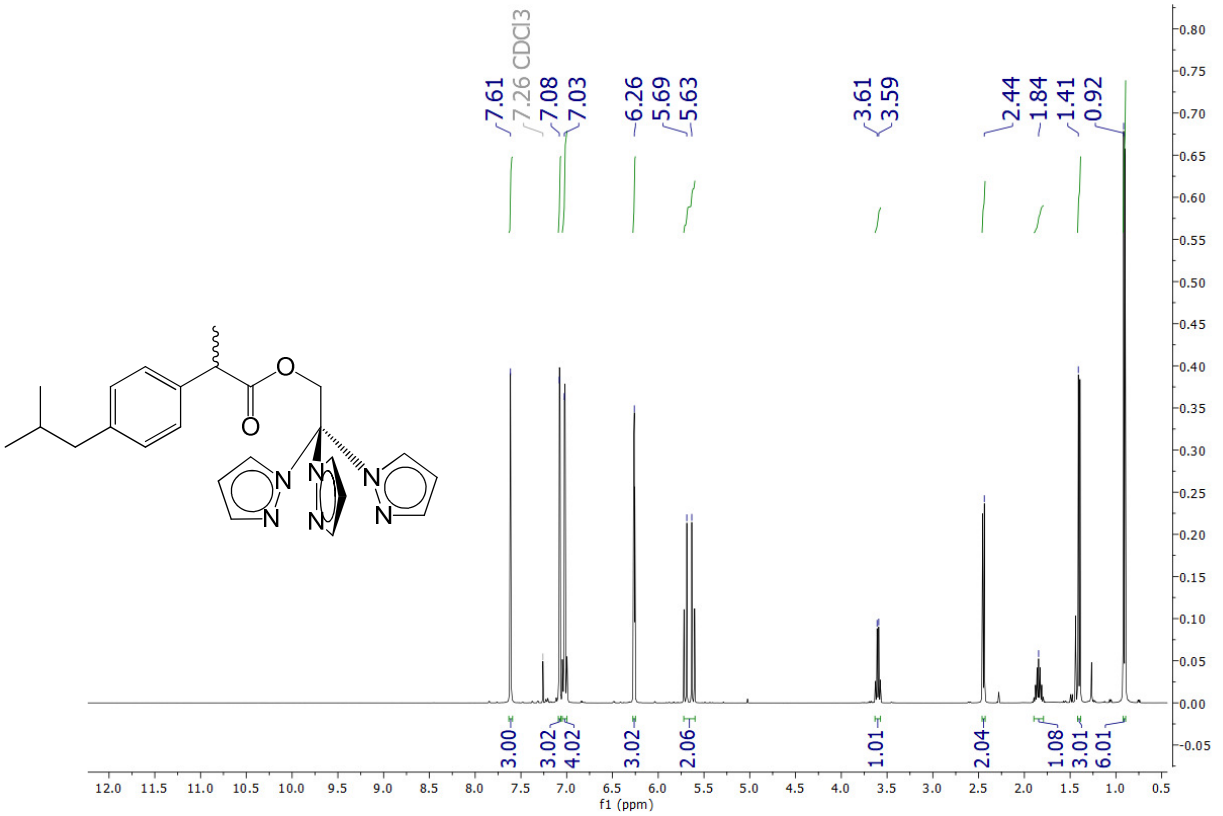

Figure S10. ^{13}C NMR spectrum (401 MHz, $CDCl_3$) of **Tpm^{IBU}**.

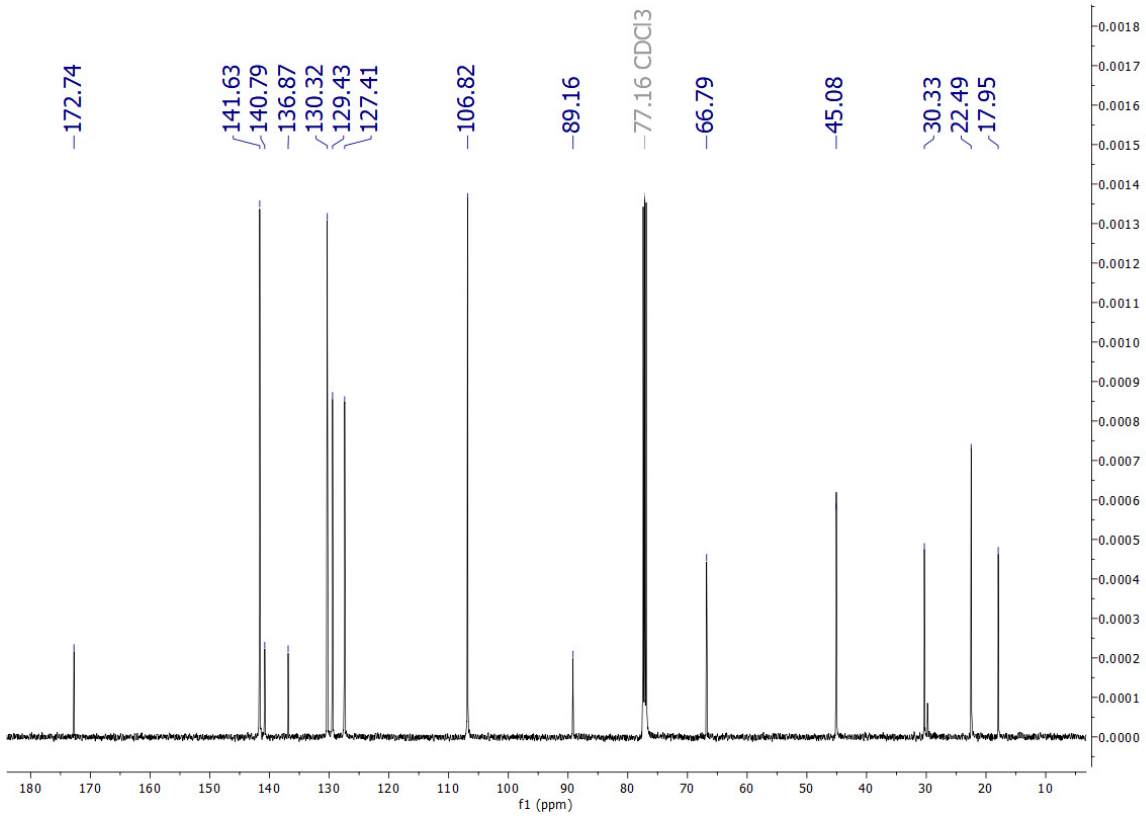

Figure S11. ^{1}H NMR spectrum (401 MHz, $CDCl_3$) of **Tpm^{FLU}.**

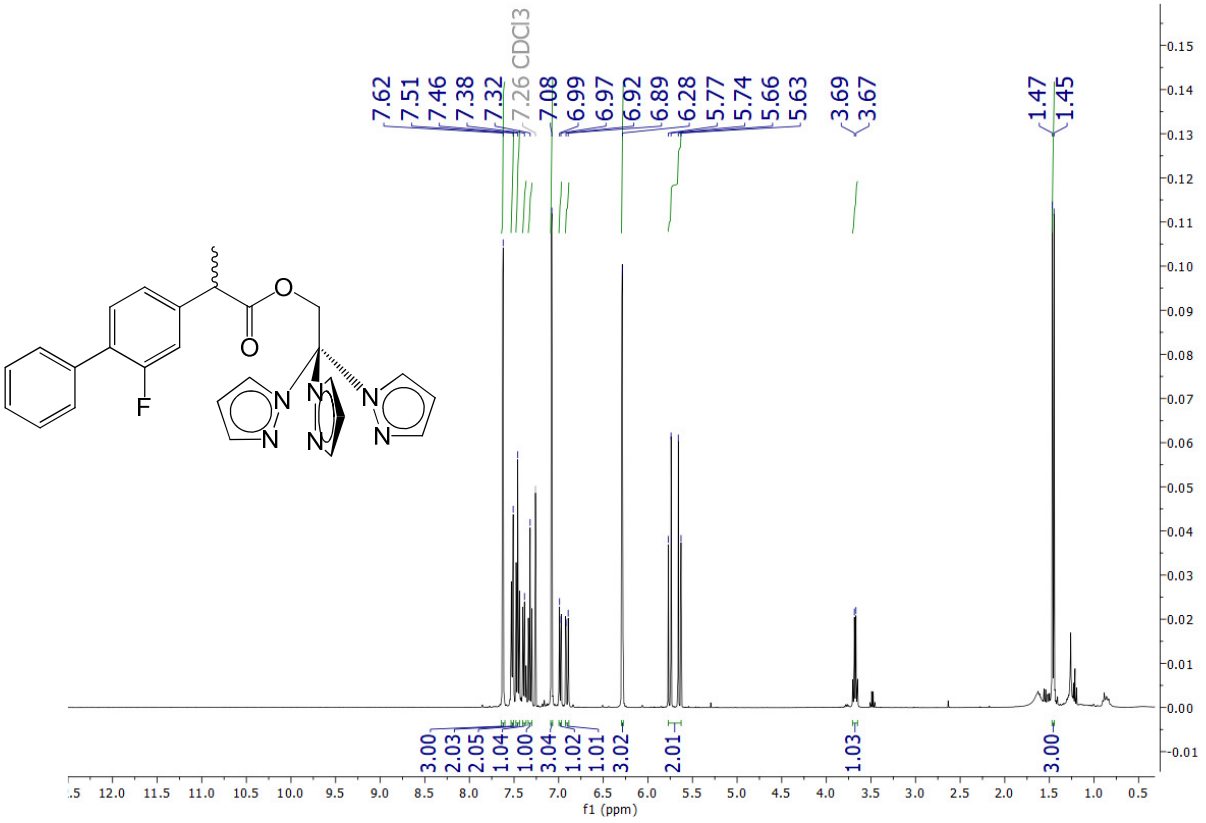

Figure S12. ^{13}C NMR spectrum (401 MHz, $CDCl_3$) of **Tpm^{FLU}.**

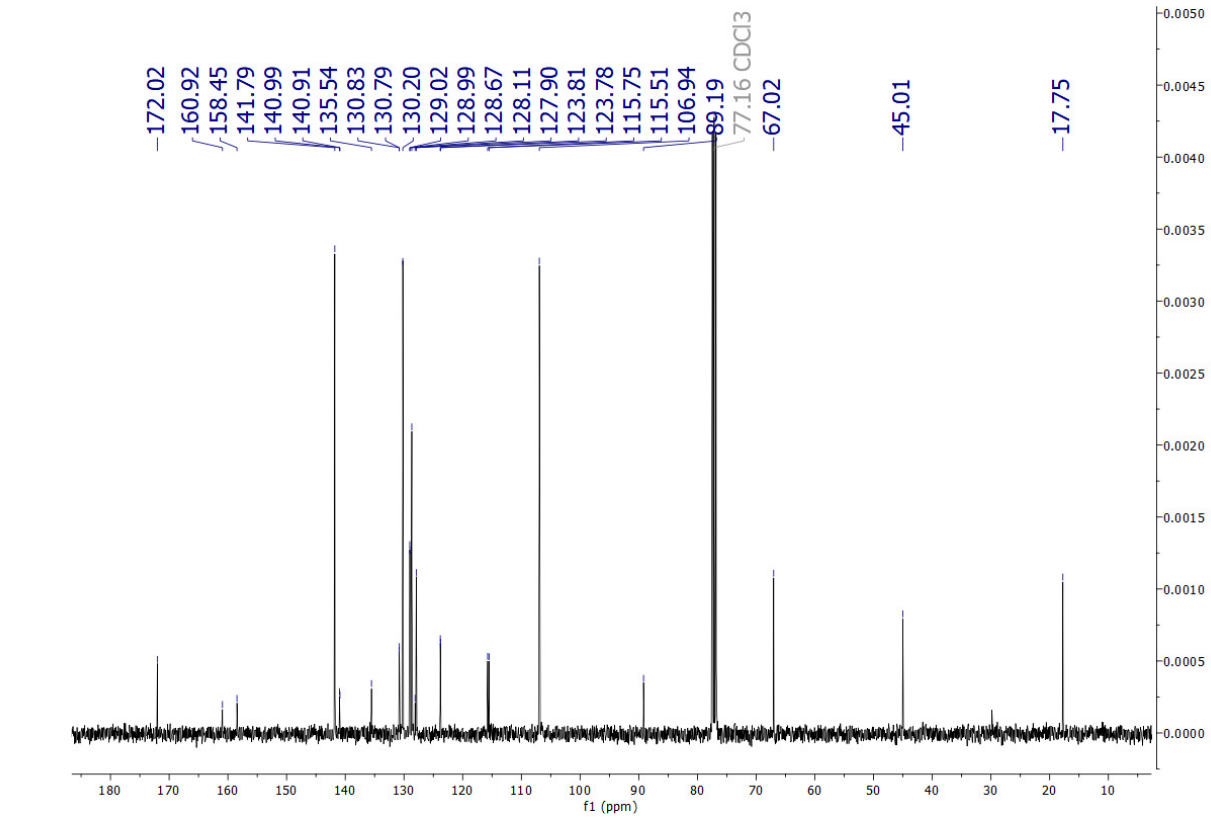

Figure S13. ^{19}F NMR spectrum (401 MHz, $CDCl_3$) of **Tpm^{FLU}.**

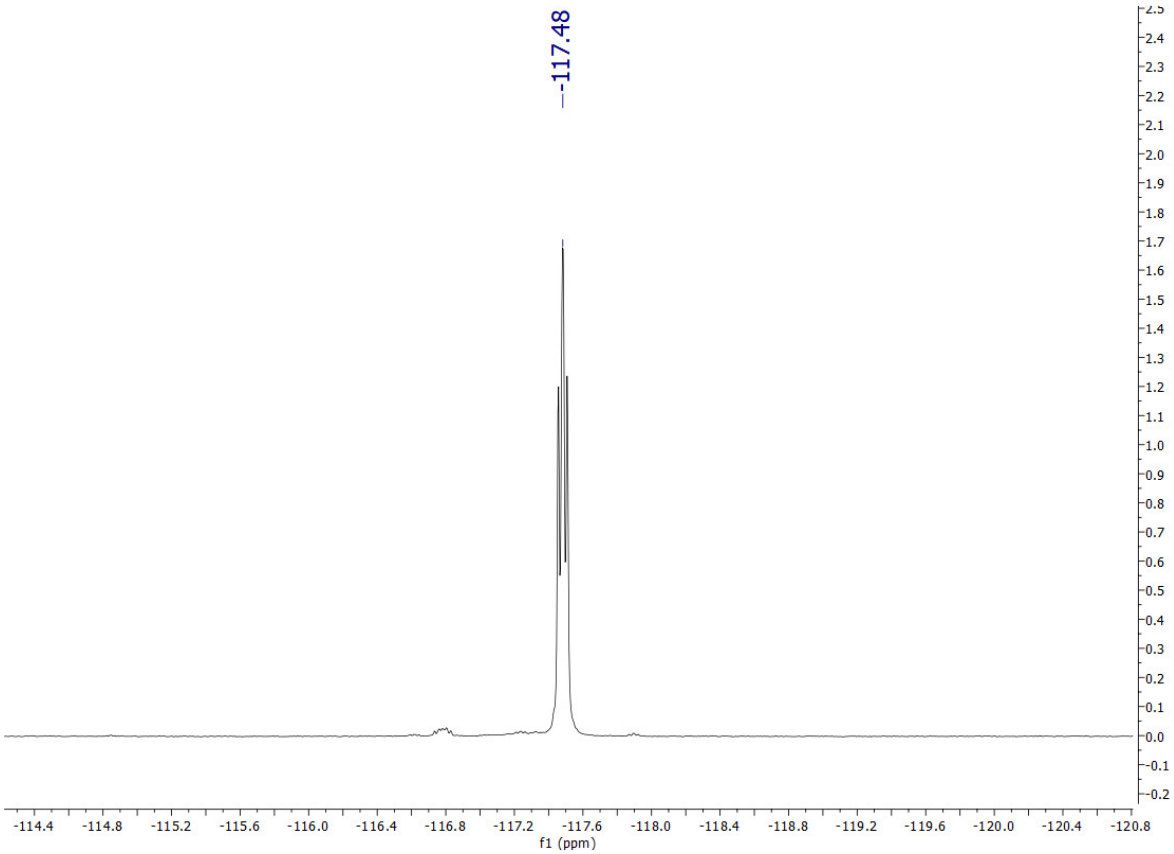

Figure S14. ^{1}H NMR spectrum (401 MHz, D_2O) of **1.**

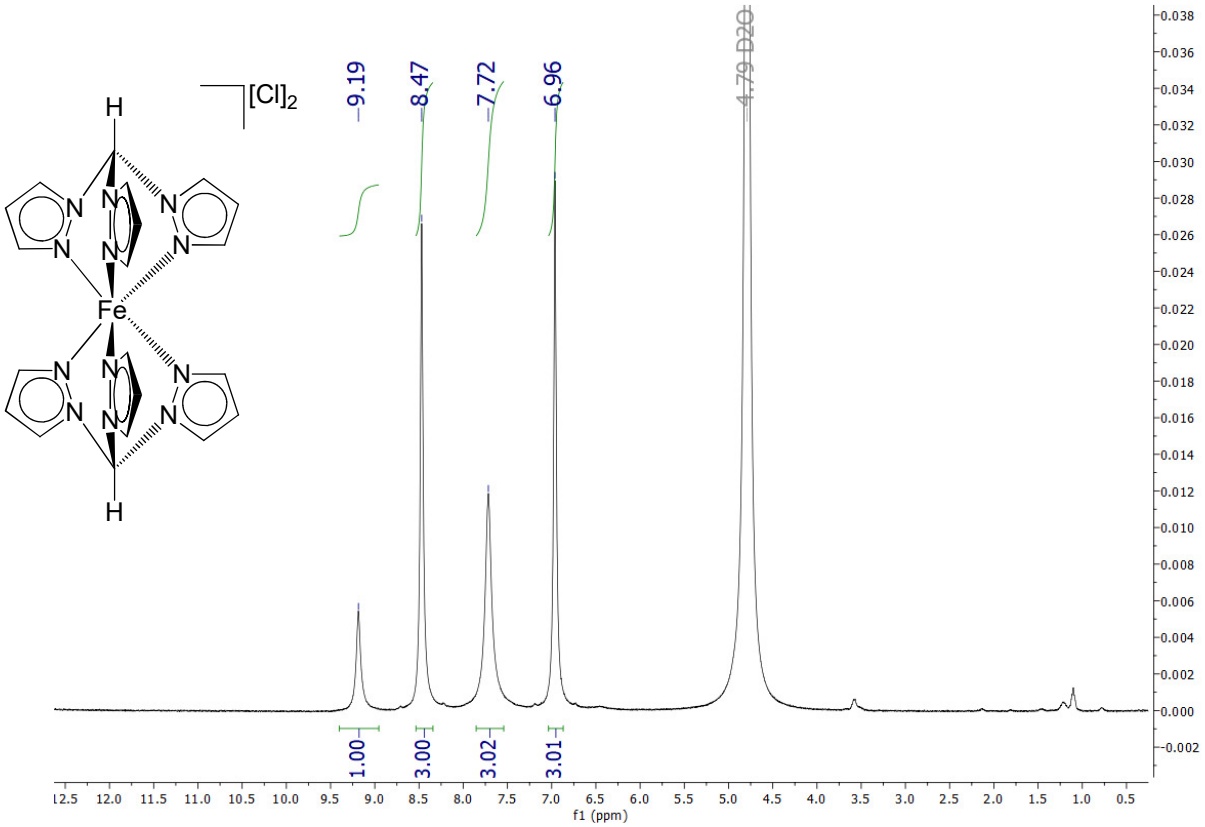

Figure S15. ^{13}C NMR spectrum (401 MHz, D_2O) of **1.**

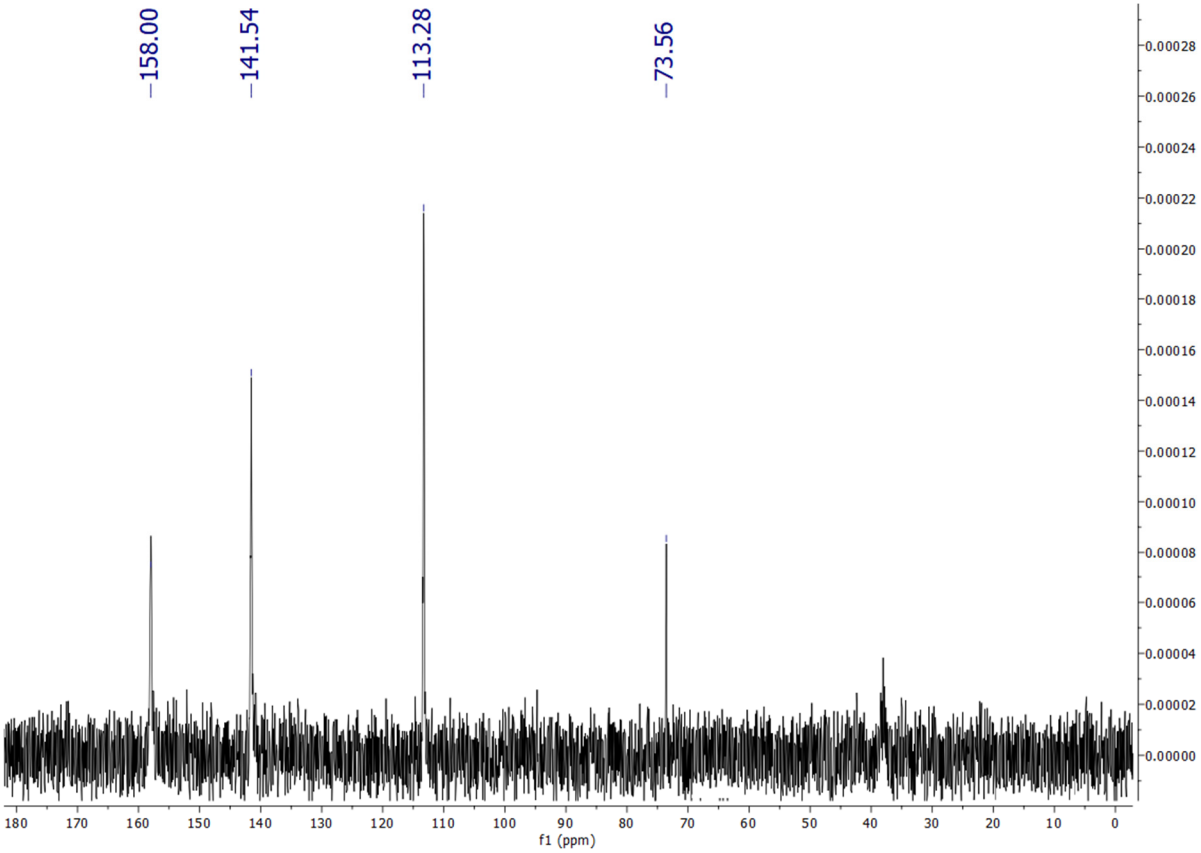

Figure S16. ^{1}H NMR spectrum (401 MHz, CD_3OD) of **2.**

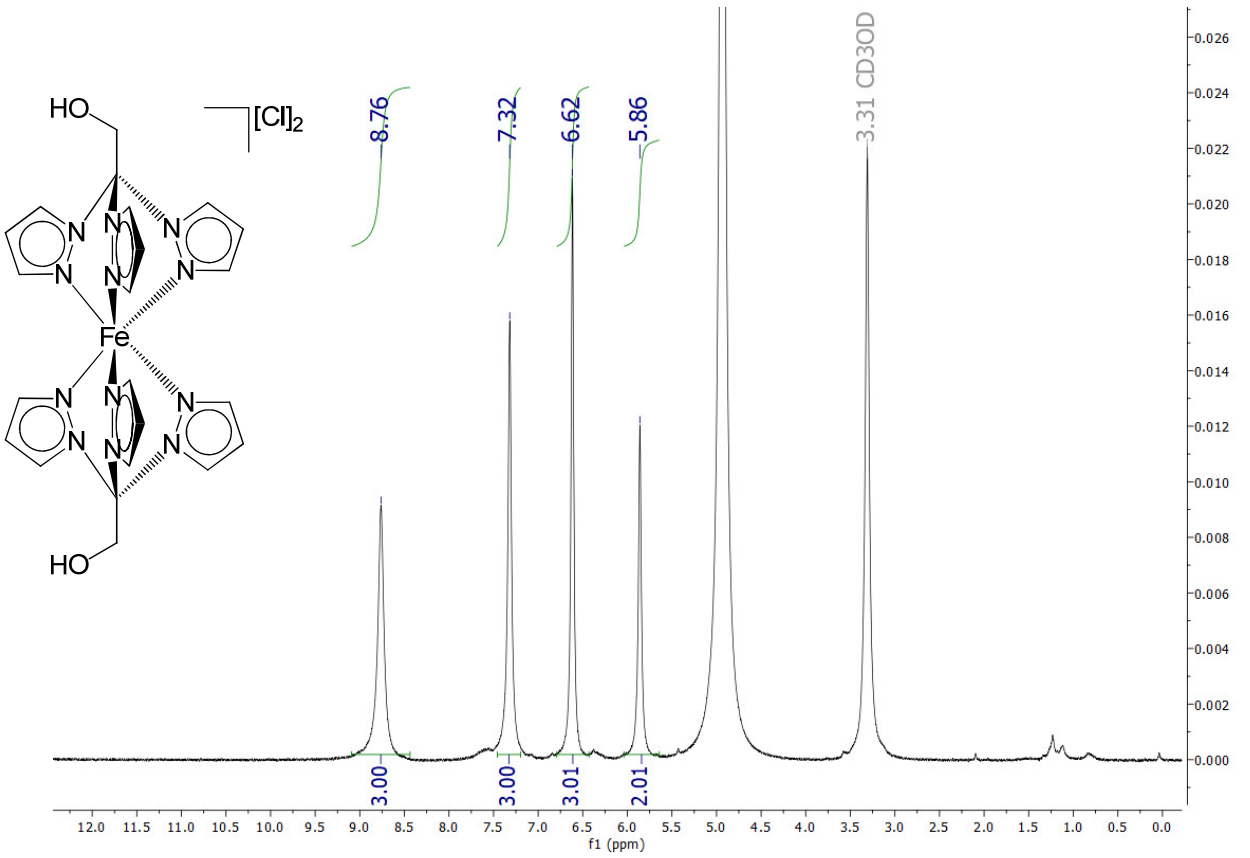

Figure S17. ^{13}C NMR spectrum (401 MHz, CD_3OD) of **2.**

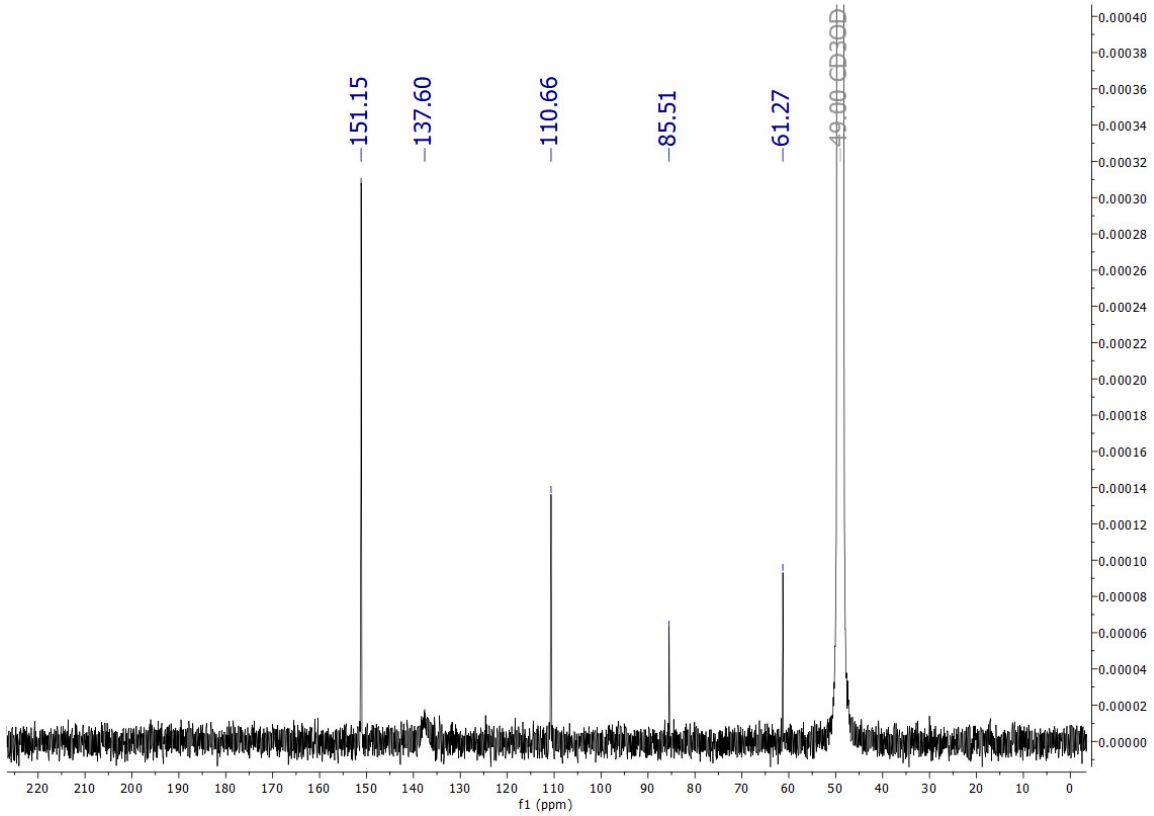

Figure S18. ^{1}H NMR spectrum (401 MHz, DMSO-d_6) of **2.**

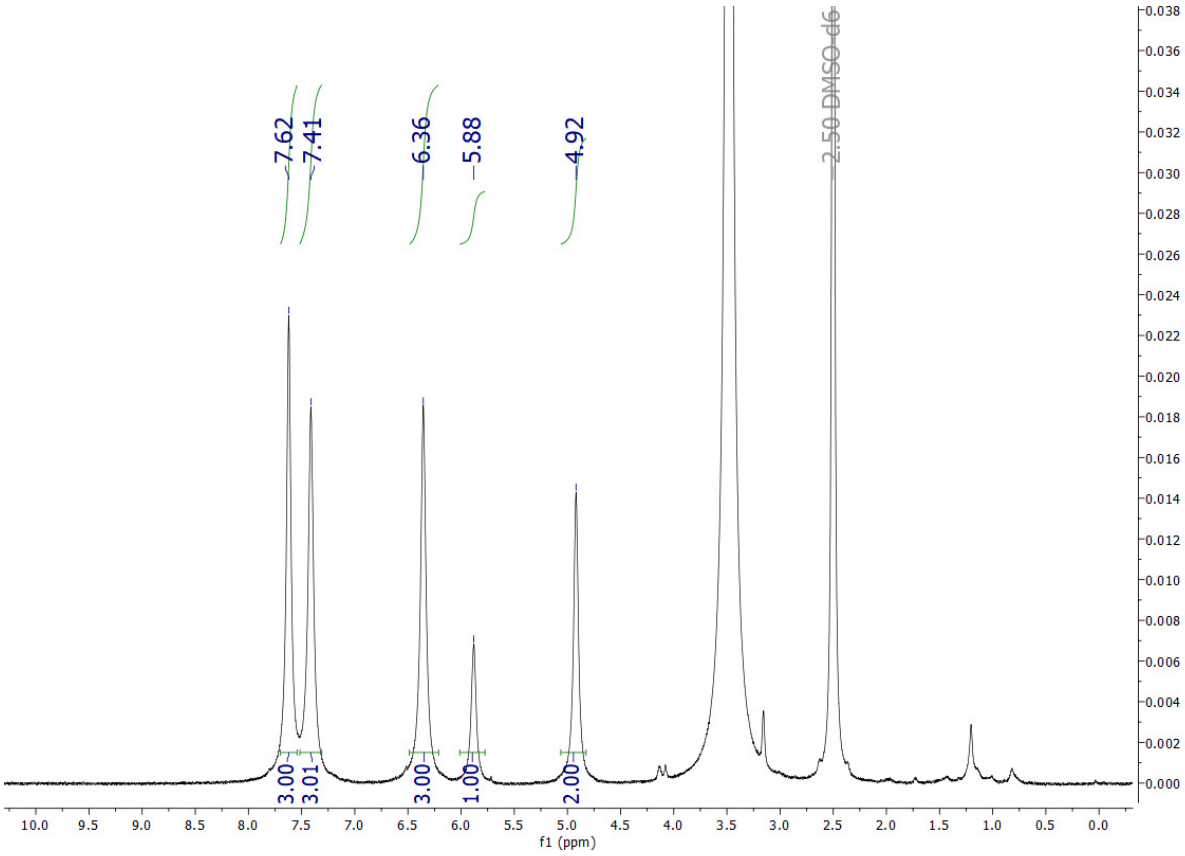

Figure S19. ^{13}C NMR spectrum (401 MHz, DMSO-d_6) of **2.**

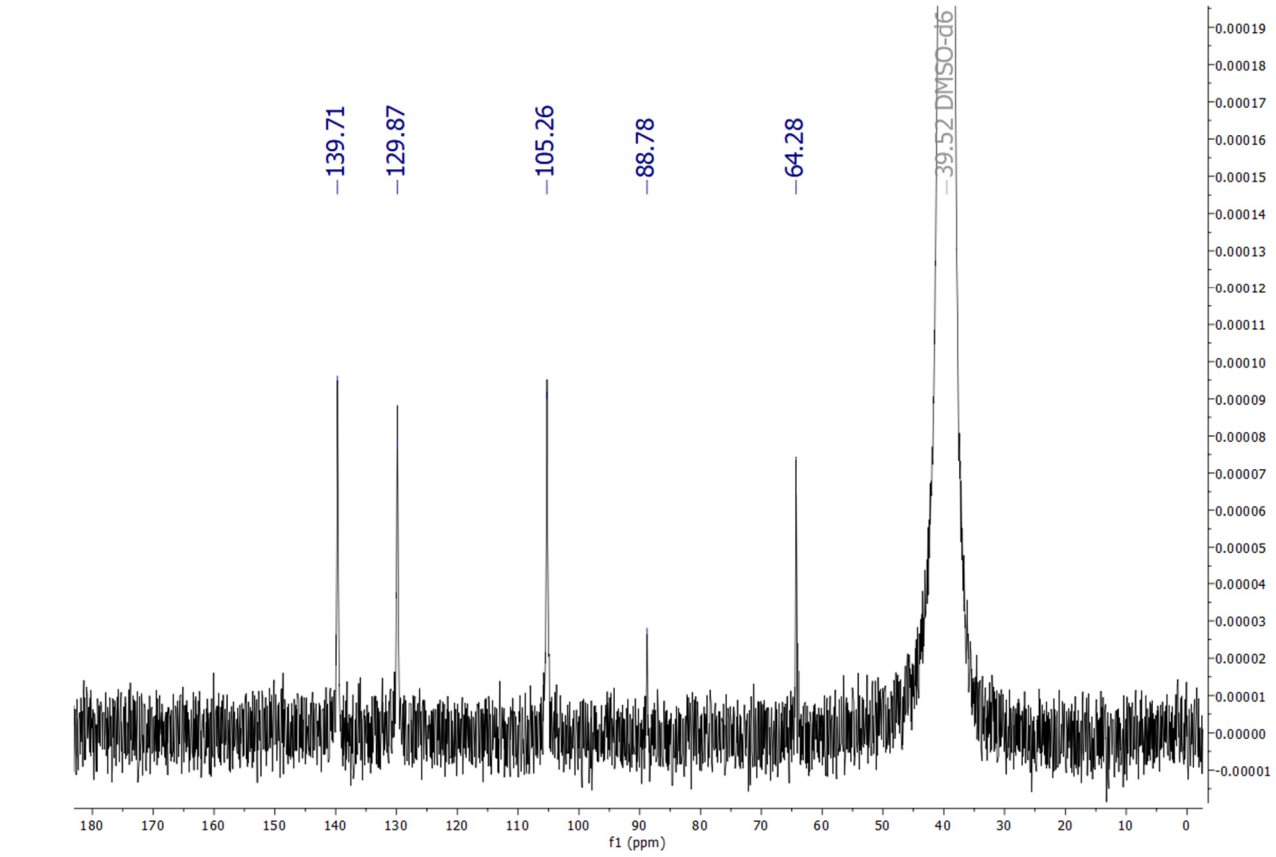

Figure S20. ^{1}H NMR spectrum (401 MHz, CD_3OD) of **3.**

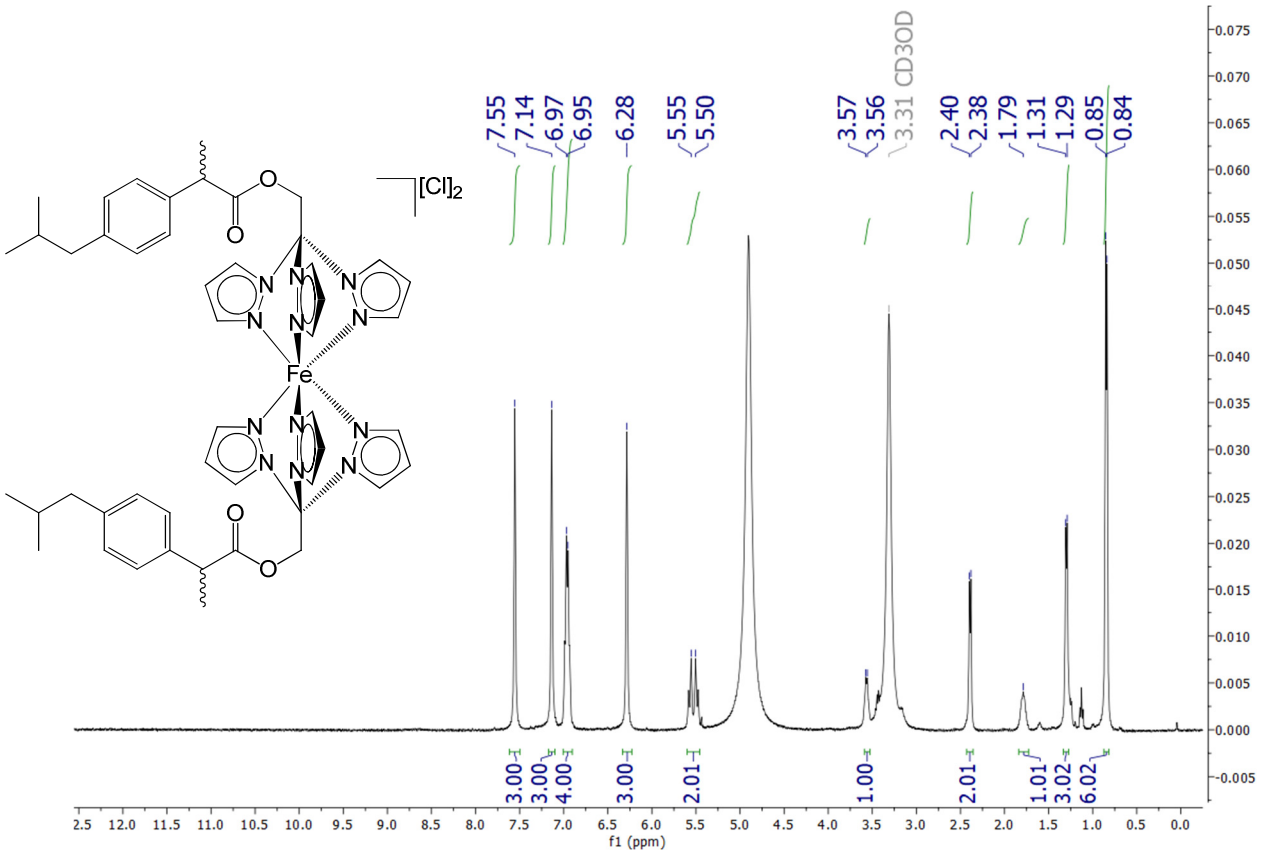

Figure S21. ^{13}C NMR spectrum (101 MHz, CD_3OD) of **3.**

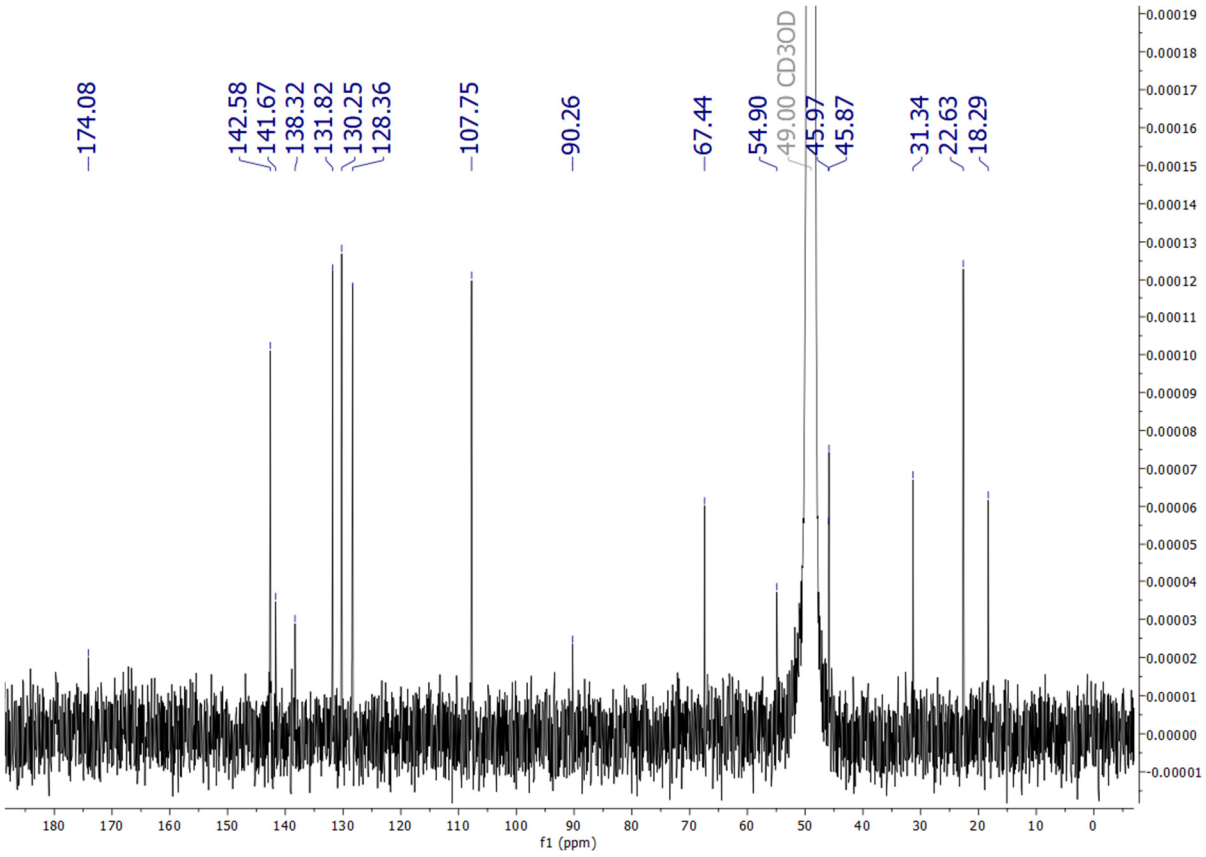

Figure S22. ^{1}H NMR spectrum (401 MHz, CD_3OD) of **4.**

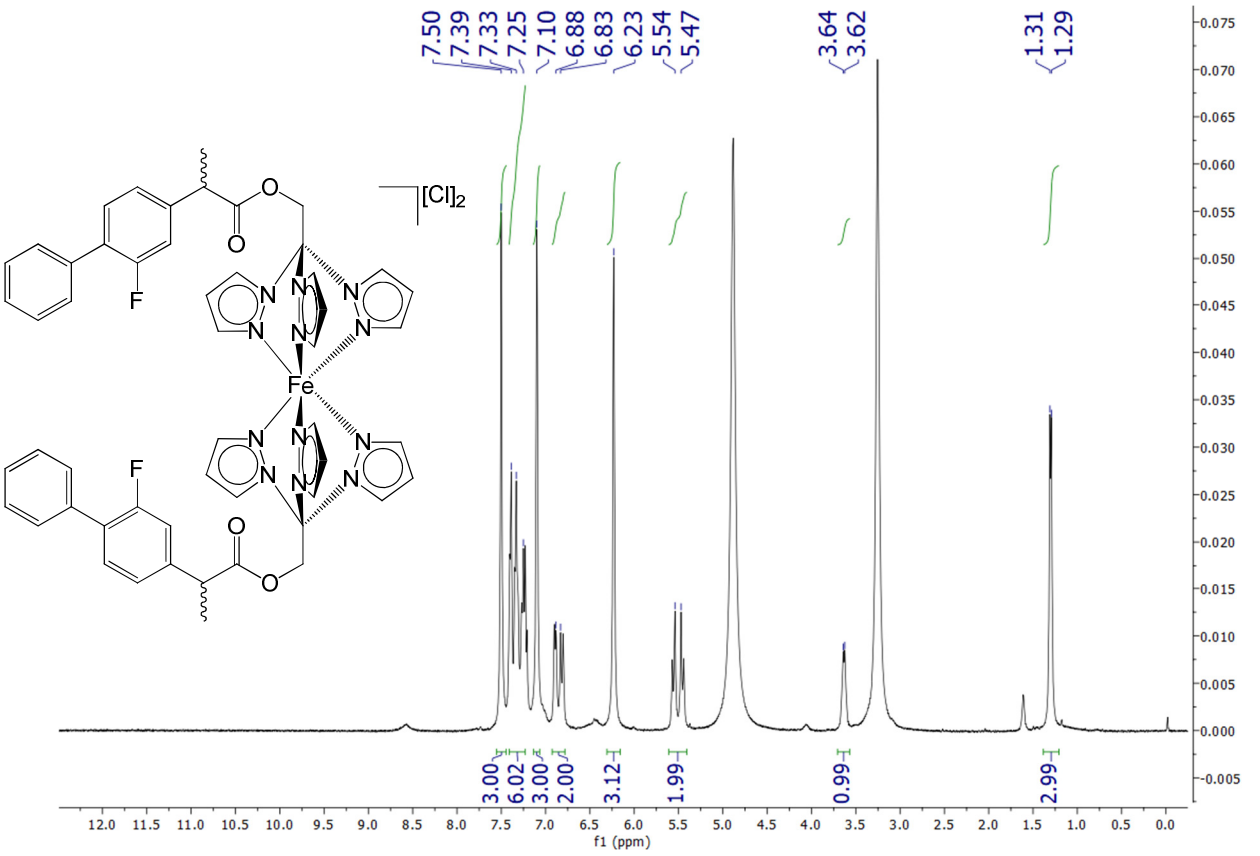

Figure S23. ^{13}C NMR spectrum (101 MHz, CD_3OD) of **4.**

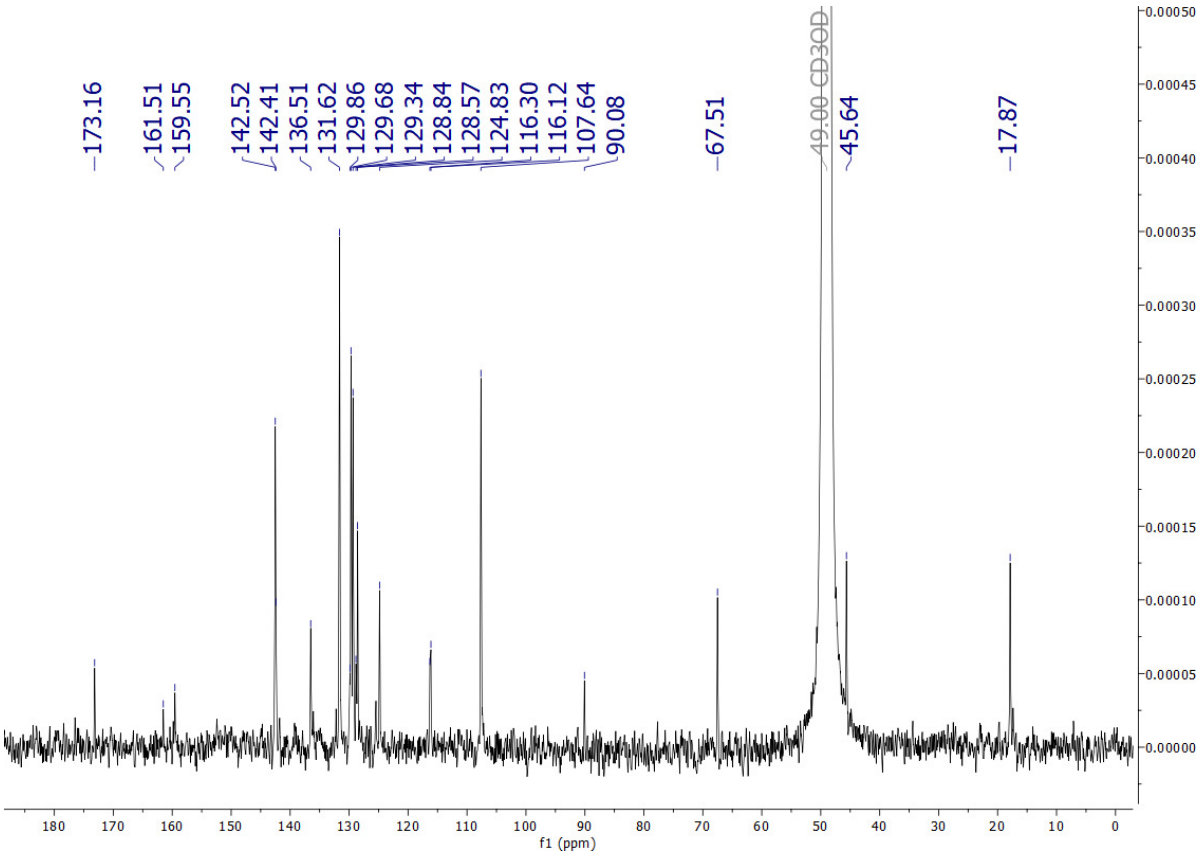

Figure S24. ^{19}F NMR spectrum (401 MHz, $CDCl_3$) of **4.**

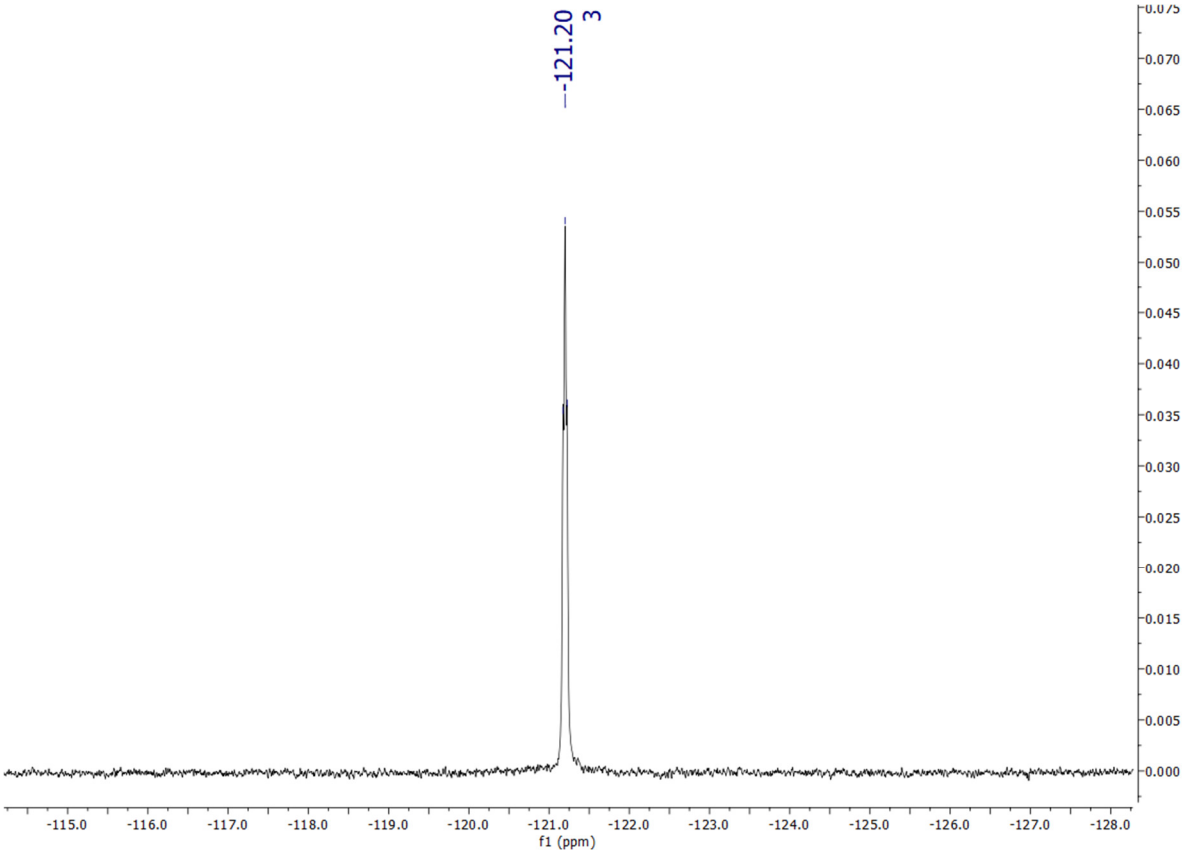

Experiments in aqueous media

a) Solubility in water. A suspension of the selected iron complex (3-5 mg) in a D_2O solution (0.7 mL) containing Me_2SO_2 as internal standard ($3.36 \cdot 10^{-3}$ M) was vigorously stirred at 21 °C for 2 h. The resulting saturated solution was filtered over celite, transferred into an NMR tube and analysed by ^{1}H NMR spectroscopy (delay time = 3 s; number of scans = 20). The concentration (solubility) was calculated by the relative integral of the starting complex with respect to Me_2SO_2 (δ/ppm = 3.14). Results are compiled in Table 1.

b) Octanol/water partition coefficients (Log P_{ow}). Partition coefficients (P_{ow}; IUPAC: K_D partition constant[3]), defined as $P_{ow} = c_{org}/c_{aq}$, where c_{org} and c_{aq} are molar concentrations of the selected compound in the organic and aqueous phase, respectively, were determined by the shake-flask method and UV-Vis measurements.[4,5] Deionized water and 1-octanol were vigorously stirred for 24 h, to enable saturation of both phases, then separated by centrifugation. A stock solution of complex **2** (*ca.* 2 mg) was prepared by first adding DMSO, (50 μL, to help solubilization), followed by octanol-saturated water (2.5 mL). The solution was diluted with octanol-saturated water (*ca.* 1:3 *v*/*v* ratio, $c_{Ru} \approx 10^{-4}$ M, so that $1.5 \leq A \leq 2.0$ at λ_{max}) and its UV-Vis spectrum was recorded (A^0_{aq}). An aliquot of the solution (V_{aq} = 1.2 mL) was transferred into a test tube and water-saturated octanol ($V_{org} = V_{aq}$ = 1.2 mL) was added. The mixture was vigorously stirred for 20 min at 21 °C then centrifuged (5000 rpm, 5 min). The UV-Vis spectrum of the aqueous phase was recorded (A^f_{aq}) and the partition coefficient was calculated as $P_{ow} = (A^0_{aq} - A^f_{aq})/A^f_{aq}$ where A^0_{aq} and A^f_{aq} are the absorbance in the aqueous phase before and after partition with the organic phase, respectively.[4c] Unfortunately, the same method did not allow the Log P_{ow} of **1** to be determined. Although this compound is substantially inert in octanol-saturated water at room temperature, as no relevant changes were observed in the UV-Vis spectrum over 2 h, the same technique indicated fast, extensive degradation upon addition of water-saturated octanol. The absence of precipitate in the mixture suggests that **1**, rather than undergoing repartition between the two phases, undergoes degradation in the presence of a large volume of octanol.

An inverse procedure was adopted for **3** and **4**, starting from a solution of the compound in water-saturated octanol. The partition coefficient was calculated as $P_{ow} = A^{f}_{org}/(A^{0}_{org} - A^{f}_{org})$ where A^{0}_{org} and A^{f}_{org} are the absorbance in the organic phase before and after partition with the aqueous phase, respectively. The wavelength of the maximum absorption of each compound (280 - 380 nm range) was used for UV-Vis quantitation. The procedure was repeated three times for each sample (from the same stock solution); results are given as mean ± standard deviation (Table 1). Naphthoquinone was used as a reference compound (Log P_{ow} = 1.8 ± 0.2; literature: 1.71).[6]

c) Stability in D_2O and DMSO-d_6/D_2O. Samples of **1** and **2** prepared according to the description in a) above were used in this experiment, whereas **3** and **4** were analysed in CD_3OD/D_2O solutions. The selected iron complex (2 mg) was dissolved in CD_3OD/D_2O 1:1 v/v solution (0.75 mL) containing Me_2SO_2 as standard.[7] The resulting solution was stirred at 21 °C for 5 min, filtered over celite, transferred into an NMR tube, analysed by ^1H NMR (delay time = 3 s; number of scans = 20) and then maintained at 37 °C for 48 h. After cooling to room temperature, NMR spectra were again recorded. The percentage of remaining starting complex was calculated from the signal integrations with respect to Me_2SO_2 ($c = 3.3 \cdot 10^{-3}$ mol·L^{-1}; δ/ppm = 3.14 in D_2O; δ/ppm = 3.05 in CD_3OD -d_6/D_2O 1:1 v/v).

d) Stability in cell culture medium. Powdered DMEM cell culture medium (1000 mg/L glucose and L-glutamine, without sodium bicarbonate and phenol red; D2902 - Merck) was dissolved in D_2O (10 mg/mL), according to the manufacturer's instructions. The solution of deuterated cell culture medium ("DMEM-d") was treated with Me_2SO_2 ($6.6 \cdot 10^{-3}$ M) and NaH_2PO_4 / Na_2HPO_4 (0.15 M, pD = 7.5),[8] then stored at 4 °C under N_2. The same procedure reported for c) above was followed for the preparation and analysis of the samples, using DMEM-d for **1** and **2**, and CD_3OD/DMEM-d 1:1 v/v for **3** and **4**. The percentage of starting complex was calculated by signal integration with respect to the reference Me_2SO_2 (δ/ppm = 3.14 in DMEM-d; δ/ppm = 3.07 in CD_3OD/DMEM-d 1:1 v/v).

NMR spectra in aqueous solutions

Figure S25. ^{1}H NMR spectrum (401 MHz, D_2O) of **2.**

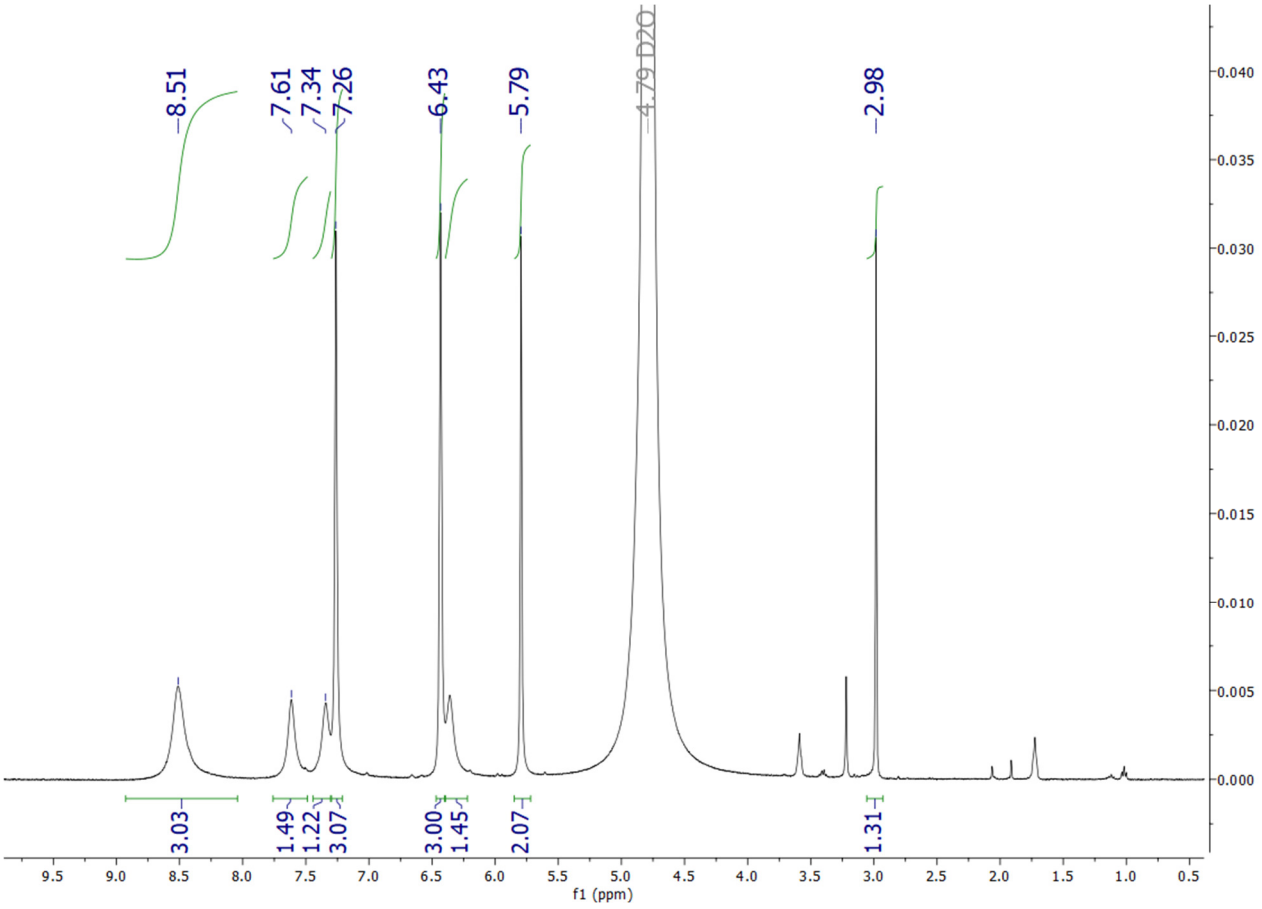

Figure S26. ^{1}H NMR spectrum (401 MHz, CD_3OD/D_2O 1:1 v/v) of **3.**

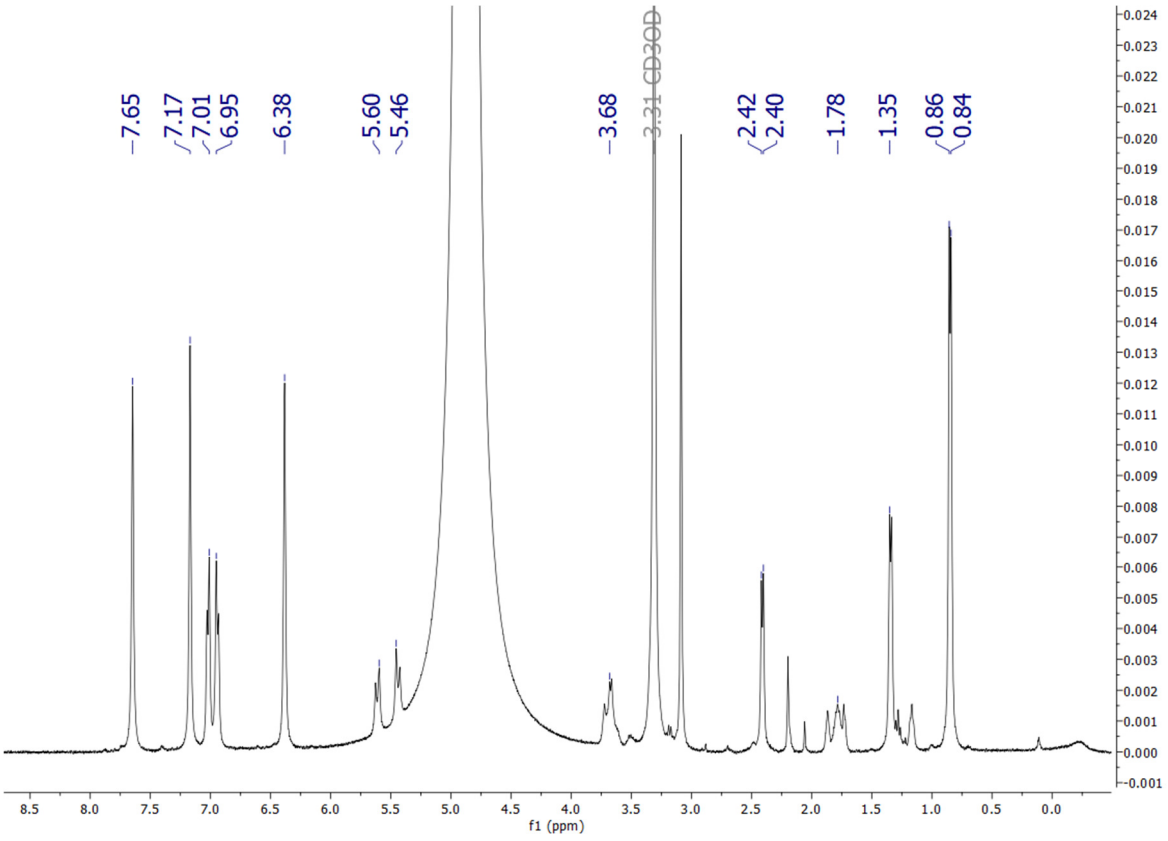

Figure S27. ^{1}H NMR spectrum (401 MHz, CD_3OD/D_2O 1:1 v/v) of **4.**

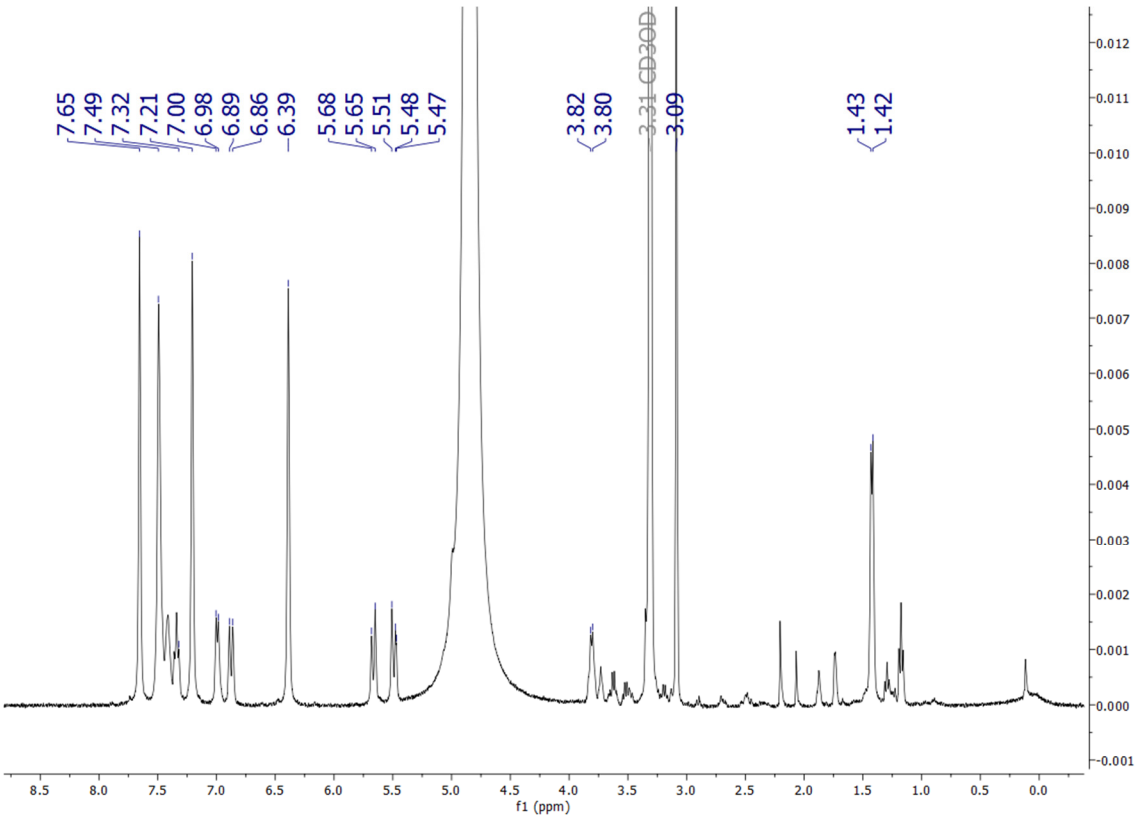

Figure S28. Absorbance decrease (F/F^0 %) observed upon addition of the metal complex **4** to the DNA/EB mixture in aqueous buffer; $C_{DNA} = 1.82\times10^{-4}$ M, $C_{EB} = 3.32\times10^{-5}$ M; titrant is $C^0_4 = 2.06\times10^{-3}$ M in DMF; aqueous buffer = NaCl 0.1 M, NaCac 0.01 M, pH = 7.0; DMF v/v% from 0 to 5.2% maximum, T = 25.0 °C, λ_{exc} = 520 nm, λ_{em} = 583 nm, F^0 is the fluorescence read at zero addition of **4**, correction for dilution factors has been considered for F. Blank test means addition of DMF only, exactly at same v/v% than the corresponding experimental point.

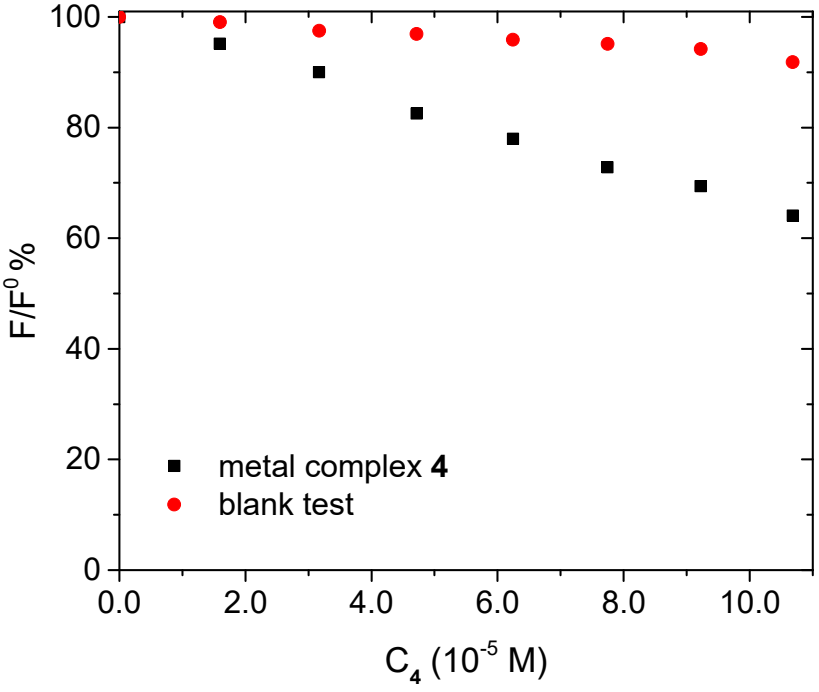

References

1 G. M. Sheldrick, SADABS-2008/1 - Bruker AXS Area Detector Scaling and Absorption Correction, Bruker AXS: Madison, Wisconsin, USA, 2008.

2 G. M. Sheldrick, *Acta Cryst. C* 2015, **71**, 3.

3 N. M. Rice, H. M. N. H. Irving and M. A. Leonard, *Pure Appl. Chem*. 1993, **65**, 2373-2396.

4 L. Biancalana, L. K. Batchelor, T. Funaioli, S. Zacchini, M. Bortoluzzi, G. Pampaloni, P. J. Dyson and F. Marchetti, *Inorg. Chem.* 2018, **57**, 6669-6685.

5 a) OECD Guidelines for Testing of Chemicals, in OECD, Paris: 1995; Vol. 107. b) J. C. Dearden, G. M. Bresnen, *Quant. Struct.-Act. Relat*. 1988, **7**, 133-144.

6 D. J. Currie, C. E. Lough, R. F. Silver, H. L. Holmes, *Can. J. Chem.* 1966, **44**, 1035-1043.

7 T. Rundlöf, M. Mathiasson, S. Bekiroglu, B. Hakkarainen, T. Bowden, T. Arvidsson, *J. Pharm. Biomed. Anal.* 2010, **52**, 645–651.

8 Calculated by the formula pD = pH* + 0.4, where pH* is the value measured for H_2O-calibrated pH-meter. a) C. C. Westcott, pH Measurements; Academic Press: New York, 1978. b) A. K. Covington, M. Paabo, R. A. Robinson and R. G. Bates, *Anal. Chem.* 1968, **40**, 700-706.